Chemical Engineering Journal 466 (2023) 143154

Contents lists available at ScienceDirect

Chemical Engineering Journal

journal homepage: www.elsevier.com/locate/cej

Electrified CO_2 valorization driven by direct Joule heating of catalytic cellular substrates

Lei Zheng, Matteo Ambrosetti, Alessandra Beretta, Gianpiero Groppi, Enrico Tronconi *

Laboratory of Catalysis and Catalytic Processes, Dipartimento di Energia, Politecnico di Milano, Via Lambruschini 4, 20156 Milano, Italy

ARTICLE INFO

Keywords:
Electrification
Joule heating
CO_2 valorization
Reverse water–gas shift
CO_2 reforming of methane
Open-cell foam

ABSTRACT

The growing environmental concerns have driven catalytic CO_2 valorization as a forward-looking solution to mitigate the carbon footprint of valuable chemical products. CO_2 conversion processes into synthesis gas, such as CO_2 reforming of methane (CRM) or reverse water–gas shift (RWGS), may have a strategic role for the future sustainable production of chemicals and energy carriers. However, fuel combustion to supply the heat of the associated endothermic reactions would result in unwanted CO_2 emissions, frustrating the overall objective. Electrification of the endothermic processes may represent the technological solution to such an issue. Here we report a promising approach for the direct electrification of the CO_2 reforming of methane (eCRM) and reverse water–gas shift (eRWGS) processes in washcoated structured reactors. We employ catalytically activated open-cell foams that provide optimal heat and mass transfer properties and serve as Joule heating substrates for the catalytic conversion of CO_2 via reaction with methane or hydrogen. The proposed reactor system with Joule-heated Rh/Al_2O_3-coated foam exhibited excellent catalytic and electrical stability for more than 75 h, operating up to 800 °C and approaching equilibrium conversion at high space velocity, i.e., GHSV of 600 and 100 $kNl/kg_{cat}/h$ for eRWGS and eCRM, respectively. Such a reactor concept has potential to ensure remarkably low specific energy demand for CO_2 valorization. Assuming an optimized process configuration approx. 0.7 kWh/Nm^3_{CO2} is calculated for eRWGS. By replacing fuel combustion with Joule heating driven by renewable electricity, the electrified CO_2 valorization processes provide an important approach for dealing with the intermittent nature of renewable sources by storing the energy in chemicals with a low carbon footprint.

1. Introduction

To meet the demand of a growing global population, unprecedented amounts of fossil fuels are used as a source of energy and feedstocks to produce necessary chemicals, releasing significant amounts of greenhouse gas and other pollutants. It is estimated that the energy consumption by the chemical industry reached 43 EJ/y in 2015, together with roughly 3.3 Gt CO_2eq emissions released to the environment, which however shows a constantly increasing trend [1]. As a result of the growing environmental concerns, CO_2 valorization has been proposed as a promising path to mitigate the carbon footprint of valuable chemical products (e-fuels, e-polymers, e-chemicals). In this context, the CO_2 reforming of methane (CRM, Eq. (1)) and the reverse water–gas shift (RWGS, Eq. (2)) reactions are interesting options for syngas production from captured CO_2 [2–4].

$$\text{CRM}: \ CO_2 + CH_4 \rightleftharpoons 2CO + 2H_2 \quad \Delta H_r^o = 247\,kJ/mol \tag{1}$$

$$\text{RWGS}: \ CO_2 + H_2 \rightleftharpoons CO + H_2O \quad \Delta H_r^o = 41\,kJ/mol \tag{2}$$

However, the endothermic nature of both reactions indicates that thermal energy is required to sustain them, which must be provided at high temperature to allow optimal process performances. In industrial-scale applications, the heat of reaction is typically supplied by fuel combustion: for CO_2 valorization processes this is paradoxical, negatively affecting the overall CO_2 balance. It is estimated that about half of the CO_2 emissions in the chemical industry are related to fuel combustion for heat supply [5].

To effectively mitigate the carbon footprint of CO_2 conversion routes, the primary energy source needs to be changed [6,7]. The electrification of catalytic processes is a promising concept that offers great potential to utilize excess renewable energy and mitigate CO_2 emissions [8–11].

In the context of CO_2 valorization processes, electrochemical reduction of CO_2 (CO_2R) enables the direct utilization of electric energy

* Corresponding author.
E-mail address: enrico.tronconi@polimi.it (E. Tronconi).

https://doi.org/10.1016/j.cej.2023.143154
Received 10 January 2023; Received in revised form 1 April 2023; Accepted 21 April 2023
Available online 23 April 2023

into CO_2 conversion, however, it is important to note that the solid oxide electrolyzer, i.e. the only technology approaching commercialization with over one year durability demonstrated [12], is characterized by an overall specific energy demand of 6–8 kWh/Nm^3_{CO2} [13]. On the other hand, power-to-heat approaches, such as induction heating, microwave heating and Joule heating, enable direct thermal energy supply without changing the reaction mechanism [14–16]. In principle, an intrinsically higher thermal efficiency (theoretically 100% [17]) can be expected from Joule heating as it is the only one that enables the direct transformation of electricity into thermal energy. Moreover, Joule heating is also characterized by fast dynamics and it has been proven that heat can be delivered at significantly high temperatures [18–20]. Process environmental and economic calculations suggest that Joule-heated CO_2 utilization processes based on renewable electricity are promising to reduce the carbon footprint of chemical products in the near future [21,22].

From the reactor engineering standpoint, one key issue is how to implement Joule heating in the design of electrified catalytic reactor. It is possible to directly heat up conductive catalyst pellets by Joule effect [23,24], however it is practically difficult to control the size of the contact area between pellets to enable electrical continuity [25]. On the other hand, the Joule heating concept is well applicable to structured catalysts, whose continuous solid matrix can ensure electrical continuity. For example, it is feasible to adopt catalytically activated commercial heating resistances with different shapes located inside the reactor [26–28], or integrate the electrical resistances (heating wires) within the channels or the framework of ceramic honeycomb monolith catalysts [29,30]. Joule heating can also be directly applied to the reactor tube, washcoated with catalyst on the inner wall [8,31]. Such configurations ensure excellent heat transfer, since the heat source is directly in contact with the catalyst; however, they are associated with significant external mass transfer limitations [32]. As an alternative solution, Joule-heated open-cell foams, characterized by high specific surface areas and excellent transport properties, have potential to overcome heat and mass transfer limitations in the electrified reactors [33–37].

These considerations motivated us to explore the electrified CO_2 reforming of methane (eCRM) and the electrified reverse water–gas shift (eRWGS) reactions by direct Joule heating of catalytically-activated open-cell SiC foams. In the present work, the Joule heating performance, catalytic performance, energy performance and CO_2 valorization performance of the electrified reactor were assessed for the eCRM and eRWGS processes.

2. Materials and methods

As in previous works from our group [33,37], the adopted SiSiC foam (d_{foam} = 3.2 cm, Erbicol, CH) has a cell diameter (d_{cell}) of 3.32 mm and a strut diameter (d_{strut}) of 0.61 mm, a total porosity estimated by ethanol picnometry of 0.88, and a surface to volume ratio evaluated on the bare geometry (Sv) of 740 m^{-1} [33]. The bulk foam material was characterized by X-ray diffraction: the analysis showed that both Si and SiC phases are present. In this work, SiSiC foams with length of 9.9 cm and 8 cm were utilized.

Rh-based catalysts are reported to be active for both reforming and reverse water-shift reactions, and have also demonstrated remarkable ability to resist coking even in demanding conditions such as CO_2 reforming of methane. [38–41]. In order to activate the SiSiC foam for catalytic reactions, a 1% Rh/Al_2O_3 catalyst was prepared in a first step via a wet-impregnation method using γ-Al_2O_3 powder (Sasol, PURALOX) as morphological support and rhodium (III) nitrate solution (Rh 10–15% w/w, Alfa Aesar) as rhodium precursor [33,37]. Afterwards, a washcoating slurry was prepared by mixing the catalyst powders with PVA (polyvinyl alcohol, Sigma-Aldrich), glycerol (Sigma-Aldrich) and deionized water via magnetic stirring and ball-milling (50 rpm) for 24 h. The SiSiC foam washcoating was achieved by dipping the foam in the catalyst slurry, followed by spinning (1000 rpm for 10 s) to remove the excess material and by flash drying in oven at 350 °C for 5 min. More details on the catalyst/slurry preparation and foam washcoating procedures can be found in our previous works [33,37]. The obtained catalytic activated SiSiC foams are shown in SI (Section S1, Fig. S1 and Fig. S2).

As shown in Fig. 1, the washcoated SiSiC foam was placed inside a tubular stainless-steel reactor (OD = 5 cm), as previously described [33,37]. The SiSiC foam was connected through electric contactors to an AC rheostat (V_{max} = 50 V, I_{max} = 100 A, Belotti Variatori) hooked to the electric grid (230 V, 50 Hz). The rheostat allowed to vary the voltage and measure the current intensity. A ceramic tube (ID = 3.5 cm) was inserted between the foam and the stainless-steel reactor tube to insulate the system. To connect the foam with the AC power generator, home-made electric contactors were adopted, these elements are made of stainless-steel cylindrical plates, provided with some holes for gas flow and welded to a ¼' stainless steel pipe. A thin layer of copper foam (Alantum, pore size 800 μm, 1 mm thickness) was placed between the SiSiC foam and the electrical contactors to minimize contact resistances. Moreover, a more robust external metallic frame structure compared to previous works [33,37] was adopted to apply additional force to the electrical contactors in order to compensate the effect of their thermal expansion. K-type thermocouples, electrically insulated by ceramic thermowells (dense alumina, d_{out} = 3 mm, d_{in} = 2 mm), were placed inside the upstream and downstream electric contactors to measure the temperatures at the upper and bottom cross sections of the foam, the measured temperatures were noted as T_{up} and T_{down}, respectively. T_{cap} was measured by a fine thermocouple placed in a quartz capillary (inner diameter of 1 mm, outer diameter 2 mm) and located at 10 mm from the centerline along the radial coordinate, through the Cu felt and in direct contact with the bottom of the foam. Another sliding thermocouple (T_{slide}) was placed inside a thermowell welded at the outer reactor wall. Temperatures were measured with a resolution of 1 cm, with a total length of 15 cm equal to the reactor length.

The electrified CO_2 reforming of methane and reverse water–gas shift runs were performed at ambient pressure, at different temperatures, space velocity and feed composition. A complete list of the experimental runs is reported in SI (Section S3, Table S1 and Table S2). The gases were fed to the system individually by means of mass flow controllers (Brooks 5851). Catalytic performance at different T_{cap} temperatures was

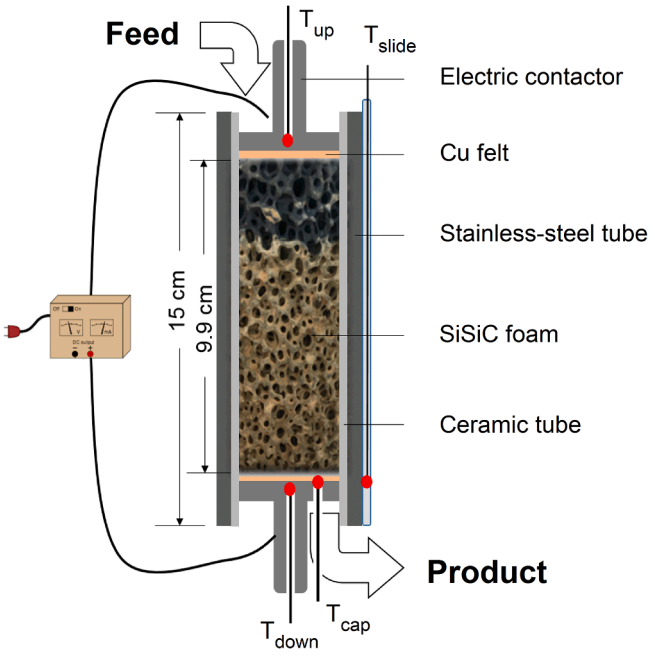

Fig. 1. Schematic representation of the electrified reactor layout. The red dots indicate where the temperatures are measured. The illustration is not to scale.

evaluated by adjusting the input voltage, the electric current self-adjusting according to the resistance of the system. The outlet gas composition was analyzed using an online micro-GC (Agilent, 900 Micro GC) after removing water from the products by a condenser. An inert gas (nitrogen) was directly fed to the micro-GC through a by-pass as an internal standard. A satisfactory closure of the carbon balance (±5%), considering CH_4, CO and CO_2 species, was obtained in all the tests. Water in the outlet stream was quantified according to the extents of reaction calculated by considering the other measured outlet species.

3. Results and discussion

3.1. Joule-heating of bare SiSiC foam

Before conducting Joule-heated catalytic experiments using catalyst washcoated SiSiC foams in a stainless-steel tube reactor, it is essential to evaluate the Joule heating performance of the bare foam. For this purpose, a quartz tube reactor was utilized to investigate the thermal behavior of the foam during the Joule heating process. Fig. 2 illustrates the Joule heating of a bare SiSiC foam loaded in a quartz tube, the foam was electrically connected through homemade contactors to an AC rheostat. To minimize contact resistances, a thin layer of copper foam was placed between the SiSiC foam and the electrical contactor. To measure the foam temperature, one thermocouple was placed inside the reactor electrically insulated by a quartz capillary and in direct contact with the foam. Another thermocouple was located outside the reactor wall.

Fig. 2 (a) shows the loaded foam at room temperature. Thanks to the interconnected geometry and suitable bulk resistivity of the SiSiC foam, it can be directly Joule heated to the relevant temperatures for electrified CO_2 reforming of methane and electrified reverse water–gas shift reactions. The adopted SiSiC foam ensures uniform power distribution and stable electrical resistance (approx. 0.3 ohm) at 700 °C in 25 Nl/h N_2 flow, as shown in Fig. 2(b).

3.2. Electrified CO_2 conversion: eCRM and eRWGS

Catalytic tests were performed by progressively increasing the electrical power input. Results in Fig. 3(a) show that the structured catalyst could be heated by the Joule effect up to the high temperatures relevant for CRM and RWGS reactions, thanks to the proper geometry and bulk resistivity of the SiSiC foam. The washcoated foam has an average catalyst layer thickness of 40 μm and a catalyst density of 39.3 g/L considering that only 4/5 of the foam volume was washcoated (Fig. S1). An almost linear correlation was observed between the input power and

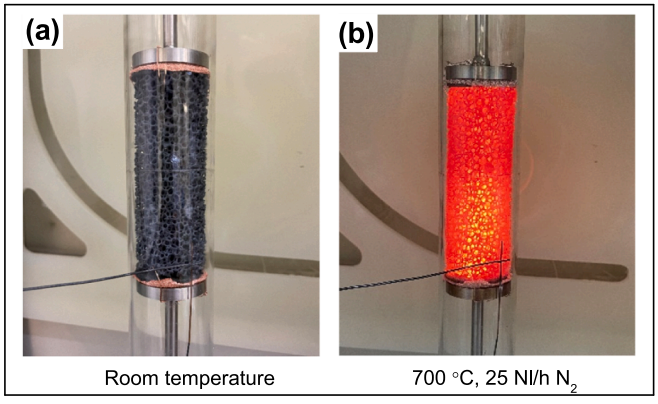

Fig. 2. Joule heating of the bare SiSiC open-cell foam (d_{foam} = 3.2 cm, L_{foam} = 9.9 cm, Erbicol, CH) in a quartz tube. (a) SiSiC foam at room temperature, the foam is connected to an AC power supplier through homemade electrical contactors. (b) Joule heated SiSiC foam with a uniform temperature distribution at 700 °C in 25 Nl/h N_2 flow, the gas flows downward from top to bottom.

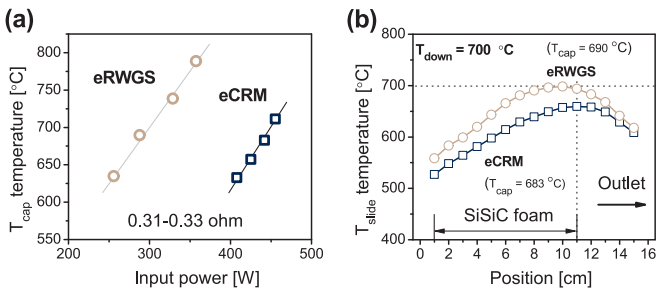

Fig. 3. Thermal performance of the electrified reactor. (a) Measured T_{cap} temperature as a function of input power during electrified CO_2 reforming of methane (eCRM) and electrified reverse water–gas shift (eRWGS) runs. (b) Axial wall temperature profiles measured by T_{slide} during eCRM and eRWGS runs at the same T_{down} temperature of 700 °C. 1 %Rh/Al_2O_3 washcoated SiSiC foam (L_{foam} = 9.9 cm) with catalyst density of 39.3 g/L. eCRM: CO_2/CH_4 = 4, GHSV = 100 kNl/kg_{cat}/h, ambient pressure. eRWGS: H_2/CO_2 = 2.25, GHSV = 100 kNl/kg_{cat}/h, ambient pressure.

the measured T_{cap} temperature.

As illustrated in (Fig. 3(b)), the axial temperature profile of the reactor wall exhibited an increasing trend along the foam length, reaching a maximum in correspondence of the foam bottom section. Such a profile is consistent with the foam acting not only as the catalyst support but also as the Joule heating element [36]. A similar trend was observed at all the investigated temperatures (Fig. S3).

The measured CO_2 conversions closely approach the thermodynamic equilibrium calculated with T_{cap} in a wide range of conditions for both eCRM and eRWGS (Fig. 4). Such a close correspondence provided us confidence that T_{cap} is well representative of the outlet temperature from the catalytic foam. The obtained results in this work were compared to the literarure reports on eCRM and eRWGS with Joule heating in Table S3.

The outlet product distribution and H_2/CO ratio reported as a function of T_{cap} (Fig. 5) confirms the close approach to equilibrium above 675 °C. Noteworthy, at these high temperature conditions any CH_4 formation could hardly be detected during eRWGS runs, in line with thermodynamics. The good catalytic performance can be attributed to the following reasons: (i) the intimate contact between the catalyst phase and the heating element results in excellent heat transfer properties compared to traditional fuel combustion heating, where heat is generated outside of the reactor; (ii) the open-cell foam provides excellent mass transfer properties due to tortuous flow in its porous structure [42].

From entalphy balances it was found that the heat dissipation, i.e., the main source of power loss, varied almost linearly with the reactor temperature (T_{cap}) and was independent from the reaction chosen (Fig. 6(a)); it was thus ascribed to heat conduction through the thermal insulation layer of the reactor and natural convection. It is important to note that the ohmic losses in the wiring increase linearly with the input power. However, these losses were estimated to account for only approximately 3% of the total power input [36,37]. As for the reaction heat duty (*Q*, Eq. S8), more energy went into the reaction in the case of the eCRM process because of its strongly endothermic nature (Fig. 6(b)). This explains why eCRM requires a higher input power to reach the same temperature in comparison to eRWGS (Fig. 3(b)). As a result, the overall energy efficiency of the system, evaluated from the ratio of process heat duty to input power (Eq. S10), reached approx. 53% for the eCRM process, which was higher compared to 25% for the eRWGS process (Fig. 6(c)). In the SI, we predictively evaluated the performances of the two systems, showing an excellent agreement in terms of temperatures, conversions and thermal efficiencies (Section S6, Fig. S4, Fig. S5 and Fig. S6). Extensive research has demonstrated that utilizing direct Joule heating of structured catalysts within the reactor yields higher energy efficiency due to more selective heating of the catalysts [18,20,43–46],

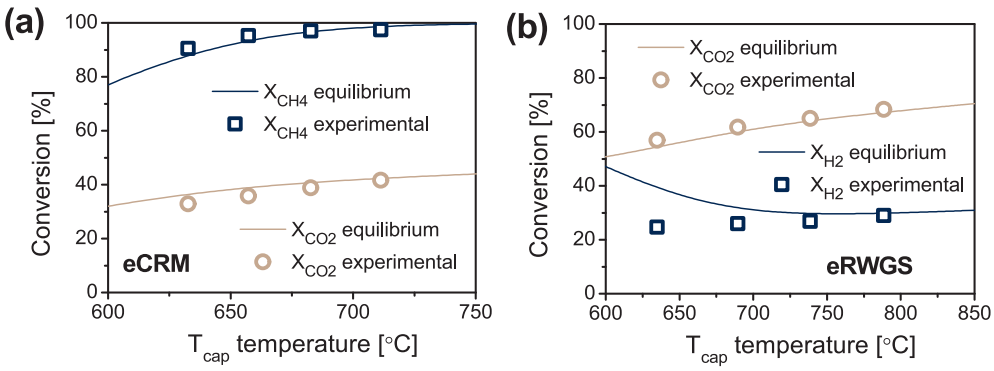

Fig. 4. Catalytic performance of the electrified reactor. (a) Measured CO_2 conversion and methane conversion as a function of T_{cap} temperature during eCRM runs. (b) Measured CO_2 conversion and hydrogen conversion as a function of T_{cap} temperature during eRWGS runs. The experimental results (dots) are compared to the thermodynamic equilibrium conversions (lines). 1 % Rh/Al_2O_3 washcoated SiSiC foam (L_{foam} = 9.9 cm) with catalyst density of 39.3 g/L. eCRM: CO_2/CH_4 = 4, GHSV = 100 kNl/kg_{cat}/h, ambient pressure. eRWGS: H_2/CO_2 = 2.25, GHSV = 100 kNl/kg_{cat}/h, ambient pressure.

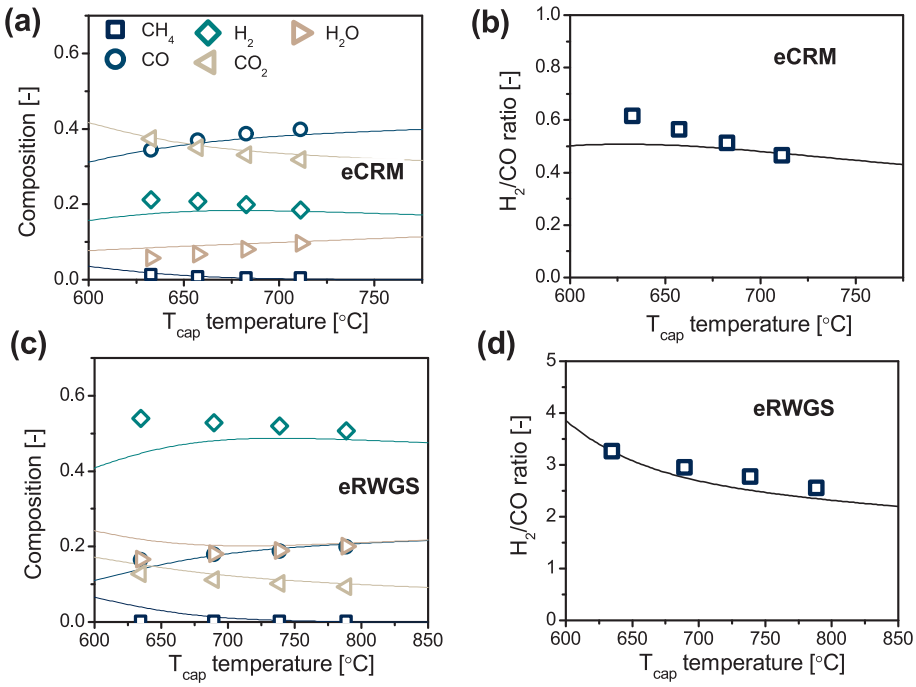

Fig. 5. (a) Outlet composition and (b) outlet H_2/CO ratio from electrified CO_2 reforming of methane (eCRM) runs. (c) Outlet composition and (d) outlet H_2/CO ratio from electrified reverse water–gas shift (eRWGS) runs. The experimental results (dots) are compared to thermodynamic equilibrium (lines). eCRM: CO_2/CH_4 = 4, GHSV = 100 000 Nl/kg_{cat}/h, ambient pressure. eRWGS: H_2/CO_2 = 2.25, GHSV = 100 000 Nl/kg_{cat}/h, ambient pressure.

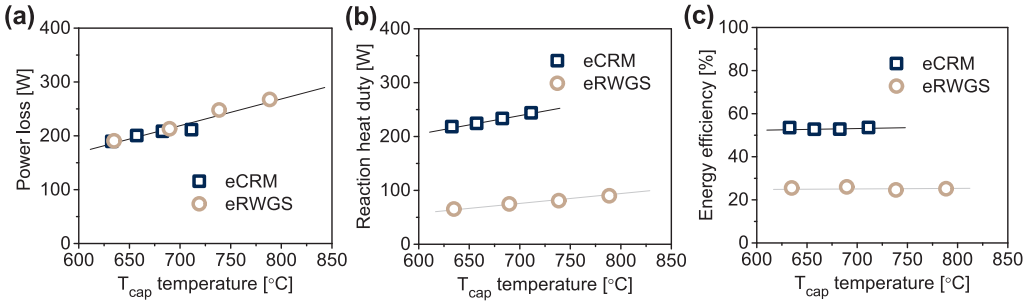

Fig. 6. Energy performance of the electrified reactor. (a) The power loss of the system as a function of measured T_{cap} temperature during electrified CO_2 reforming of methane (eCRM) and electrified reverse water–gas shift (eRWGS) runs. (b) Reaction heat duty (Q) as a function of measured T_{cap} temperature during eCRM and eRWGS runs. (c) Energy efficiency (the ratio of reaction heat duty to input power) as a function of measured T_{cap} temperature during eCRM and eRWGS runs. 1 %Rh/Al_2O_3 washcoated SiSiC foam (L_{foam} = 9.9 cm) with catalyst density of 39.3 g/L. eCRM: CO_2/CH_4 = 4, GHSV = 100 kNl/kg_{cat}/h, ambient pressure. eRWGS: H_2/CO_2 = 2.25, GHSV = 100 kNl/kg_{cat}/h, ambient pressure.

in contrast to electric oven heating where heat is generated outside of the reactors. Further improvement of energy efficiency is still possible, for example, by increasing the total flow rate and by minimizing heat dissipations with better thermal insulation. More importantly, a significant improvement of the energy efficiency up to values close to 1 can be expected upon scale-up (Fig. S7), which facilitates quasi adiabatic operations [15,36].

The CO_2 valorization performances of the proposed foam-based

electrified reactor were evaluated based on the mole of reductant feed (CH_4 in eCRM and H_2 in eRWGS), catalyst and electrical energy inputs (Fig. 7). The eRWGS process reached a net CO_2 consumption (NC_{CO2}) of 1 mol_{CO2}/mol_{H2}, consistent with the reaction stoichiometry (CO_2/H_2 = 1, Eq. (2). In contrast, higher values of 1.3–1.6 mol_{CO2}/mol_{CH4} were achieved in the eCRM runs (Fig. 7(a)), thanks to the concurrent RWGS reaction where CO_2 (excess CO_2 as a result of CO_2 rich feed CO_2/CH_4 = 4) further reacted with the produced H_2 (Eq. (2)). The evidence for this aspect is provided by the $K_p/K_{eq\text{-}rwgs}$ ratios computed during eCRM runs: as shown in Fig. S8, all such values were below 1, confirming that the RWGS reaction is indeed favoured in eCRM conditions.

The overall CO_2 conversion rate per catalyst mass (VR_{CO2}, Fig. 7(b)) reached 20 and 31 $Nm^3_{CO2}/kg_{cat}/h$ for eRWGS and eCRM, respectively, however, higher values could be expected with the increase of the feed CO_2/reductant ratio and especially the increase of the space velocity, since the system in all the investigated conditions was at thermodynamic equilibrium.

The eCRM process enables higher net CO_2 consumptions (Fig. 7(a)) and CO_2 conversion intensities (Fig. 7(b)), however, it requires greater electric energy input to reach the target reaction temperature in comparison to the eRWGS process (Fig. 3(b)). As a result, the specific energy demand for CO_2 valorization (SE_{CO2}, Eq. S14) fell in a similar range of 5.2–6.7 kWh/Nm^3_{CO2} for both eCRM and eRWGS processes (Fig. 7(c)). The SE_{CO2} in eRWGS runs increased with input power as the heat loss played a major role at high temperatures; in contrast, a decreasing trend was observed in eCRM runs showing that a significant amount of energy was absorbed by the reaction.

The Joule-heated systems in principle enable significantly high energy efficiency [17]. Mathemathical model simulations demonstrated that approx. 95% efficiency can be reached in a 0.12 m diameter, 1.25 m long e-RWGS reactor operated at GHSV = 150 $kNl/kg_{cat}/h$ with an input power density of 6.5 MW/m^3 (SI, Fig. S7), therefore based on this figure (η^* = 0.95) we calculate a quasi adiabatic specific energy (SE^*_{CO2}, Eq. S15) as low as 1.4 kWh/Nm^3_{CO2}. Moreover, a big advantage could be gained by recovering the large fraction of sensible heat, i.e., by pre-heating the reactants, especially for eRWGS process ((Fig. 7(e)). In view of this, a second process integrated specific energy (SE^{**}_{CO2}, Eq. S18), evaluated by further considering the recover of 90% sensible heat [47], reached approx. 0.7 kWh/Nm^3_{CO2} for eRWGS. In the eRWGS process, if the feed H_2 is sourced from water electrolysis (3.8 kWh/Nm^3_{H2}) [48,49], it is possible to achieve an overall specific energy consumption of 4.5 kWh/Nm^3_{CO2} for CO_2 valorization when operating with a recycle reactor. Such results are very attractive compared to solid oxide electrolyzers for CO_2 reduction (6–8 kWh/Nm^3_{CO2}, [13]).

Since more energy is required to activate CH_4 than H_2 [3], the eCRM was observed to show higher SE^{**}_{CO2} values (2.3–2.6 kWh/Nm^3_{CO2}) compared to eRWGS processes. In addition to CO_2 valorization, the eCRM process could be regarded as an environmental-friendly approach to activate methane. The decreasing trend of SE^{**}_{CO2} with temperature in eCRM runs could be explained by the concurrent RWGS reaction ((Fig. 7 (a)). This suggests that the SE^{**}_{CO2} is dependent on the feed gas composition and operating temperature, therefore further reduction of this value is in principle feasible, e.g., by feeding a more CO_2-rich gas mixture.

3.3. eRWGS: Effect of H_2/CO_2 feed ratio

As indicated by thermodymamics (*c.f.* equilibrium curves of Fig. 4), increasing the power input (and temperature) would have a positive, but limited effect on improving the CO_2 conversion during eRWGS runs. On the other hand, as previously discussed, the CO_2 conversion could be

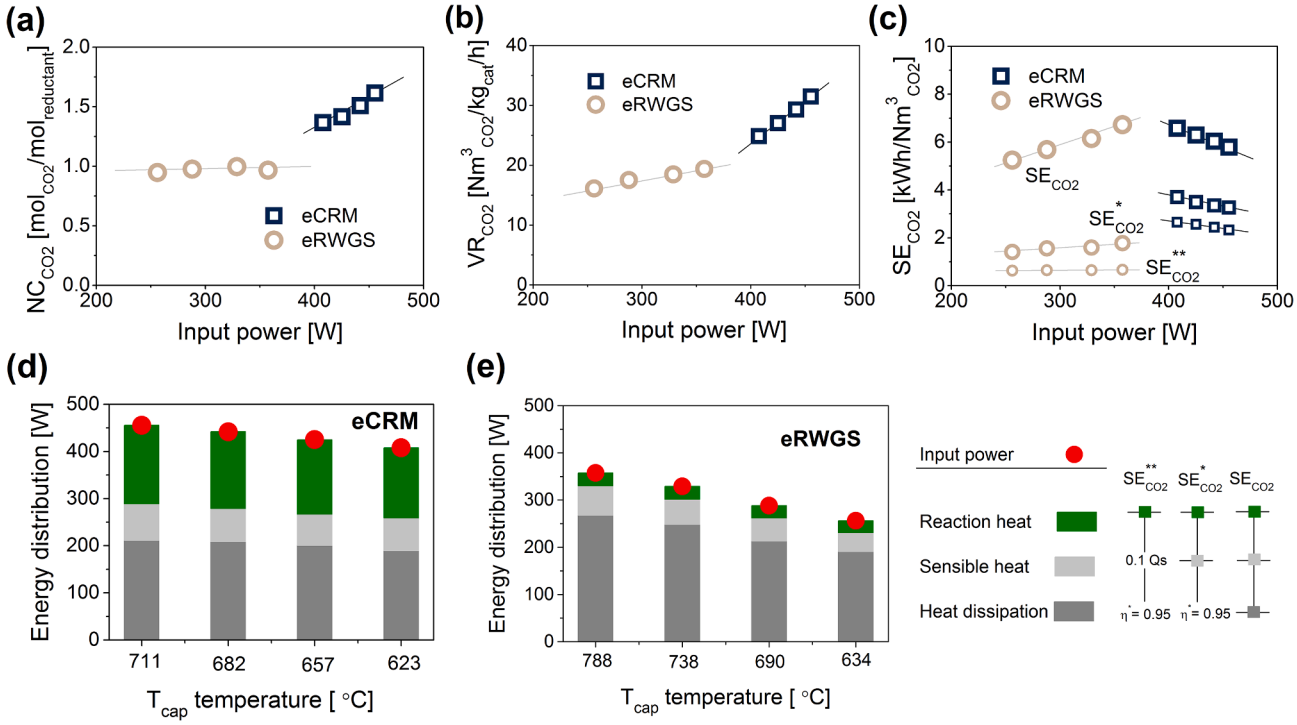

Fig. 7. CO_2 valorization performance of the electrified reactor. (a) Net CO_2 consumption per mol of converted reductant (NC_{CO2}) as a function of input power during electrified CO_2 reforming of methane (eCRM) and electrified reverse water–gas shift (eRWGS) processes. (b) Overall CO_2 valorization rate (VR_{CO2}) as a function of input power during eCRM and eRWGS processes. (c) Specific energy consumption for CO_2 valorization (SE_{CO2}) as a function of input power during eCRM and eRWGS processes: experimental results based on input power (SE_{CO2}), the theoretical results considering an overall energy efficiency of 95% (SE^*_{CO2}), as well as a further revover of 90% sensible heat (SE^{**}_{CO2}). The energy distribution as a function of T_{cap} temperature during (d) eCRM and (e) eRWGS runs. 1 %Rh/Al_2O_3 washcoated SiSiC foam (L_{foam} = 9.9 cm) with catalyst density of 39.3 g/L. eCRM: CO_2/CH_4 = 4, GHSV = 100 $kNl/kg_{cat}/h$, ambient pressure. eRWGS: H_2/CO_2 = 2.25, GHSV = 100 $kNl/kg_{cat}/h$, ambient pressure.

further enhanced by increasing the H_2/CO_2 feed ratio. Our experimental results of CO_2 and H_2 conversions during eRWGS runs with different H_2/CO_2 feed ratios (T_{cap} = 800 °C, GHSV = 100 kNl/kg_{cat}/h, ambient pressure) are illustrated in Fig. 8. The experiments were performed using the same 1 %Rh/Al_2O_3 washcoated SiSiC foam (L_{foam} = 9.9 cm) with a catalyst density of 39.3 g/L. CO_2 conversion consistently increase with the H_2/CO_2 feed ratio up to 94.2%, which was achieved with an H_2/CO_2 feed ratio of 20. However, it is evident that the system is constrained by thermodynamic equilibrium, and further increase the H_2/CO_2 feed ratio will not significantly enhance CO_2 conversion. Moreover, operation in these conditions is questionable, since the separation and recycle of H_2 should be considered. We envision this solution for systems where CO is the main product of interest.

3.4. eRWGS: Effect of GHSV

To further explore the eRWGS at high GHSV, we prepared another washcoated SiSiC foam (L_{foam} = 8 cm) with a low catalyst density of 13 g/L. This enabled us to operate the system up to GHSV = 600 kNl/kg_{cat}/h. The washcoated foam had an average catalyst layer thickness of 13.2 μm, considering that 4/5 of the foam volume was washcoated (Fig. S2). As shown in Fig. 9(a), under kinetic controlled conditions CO_2 conversion decreases on increasing GHSV. Expectedly, such an effect vanishes once equilibrium is reached at the reactor outlet, which occurs at progressively higher temperature on increasing the GHSV. At 700 °C equilibrium conversions were attained, even with the highest space velocity of 600 kNl/kg_{cat}/h. Fig. 9(b) compares the corresponding CH_4 outlet fraction results to equilibrium. Hardly any CH_4 was detected above 650 °C, consinstently with the equilibrium predictions. At low temperatures, lower CH_4 outlet fractions were obtained with increasing space velocity. Heyl et al. [50], reported that CH_4 was produced with CO as intermediate during CO_2 hydrogenation over Rh/Al_2O_3 catalyst. This indicates that with incrasing space velocity, the methanation reaction becomes slower compared to RWGS, in line with literature reports [31,51].

Fig. 9(c) illustrates the effect of H_2/CO_2 feed ratio on CO_2 conversion at GHSV of 600 kNl/kg_{cat}/h. The system was mainly thermodynamically controlled above 700 °C for all the investigated H_2/CO_2 feed ratios. Fig. 9(d) shows that high H_2/CO_2 feed ratios favored the CH_4 formation at low temperatures, in line with equilibrium.

To verify the stability of the system, eRWGS tests were carried out repeatedly with T_{cap} of 700 °C and 650 °C (H_2/CO_2 = 2, 600 kNl/kg_{cat}/h, ambient pressure) at different working hours (15 h, 60 h, and 75 h), as shown in Fig. 10(a). The two conditions were selected as they are representative of the thermodynamic and kinetic controlled regimes, respectively. In between those selected stability runs, we also carried out eRWGS tests at different conditions, i.e., different space velocities and H_2/CO_2 feed ratios (*c.f.* experimental log from Table S2). We found that the structured catalyst remained stable throughout the testing period, with no significant drop in either CO_2 or H_2 conversions, as shown in Fig. 10(a). Additionally, the electric resistance of the system remained almost constant at 0.32 ohm, indicating the good electric stability of the foam-based reactor. Fig. 10(b) displays photos of the fresh (left) and used (right) SiSiC foam after at least 80 h on eRWGS stream with varied conditions. We observed no significant deterioration of the catalyst layer and just a slight color change (darkening) that can be attributed to Rh reduction.

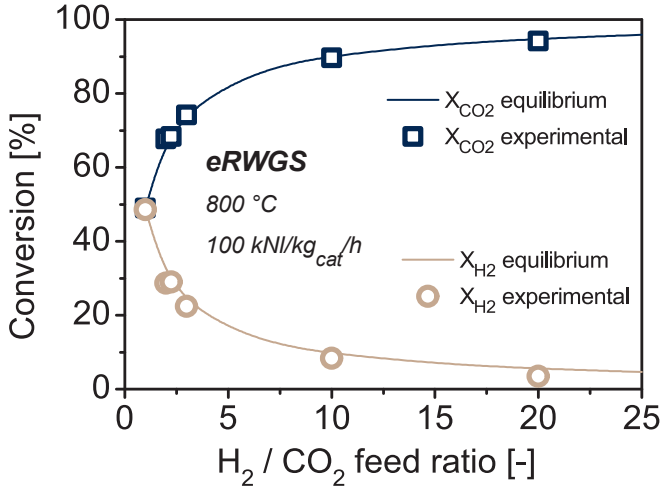

Fig. 8. CO_2 and H_2 conversions during eRWGS runs with different H_2/CO_2 feed ratios. 1 %Rh/Al_2O_3 washcoated SiSiC foam (L_{foam} = 9.9 cm) with catalyst density of 39.3 g/L. Experiments carried out at 800 °C, GHSV = 100 kNl/kg_{cat}/h, ambient pressure.

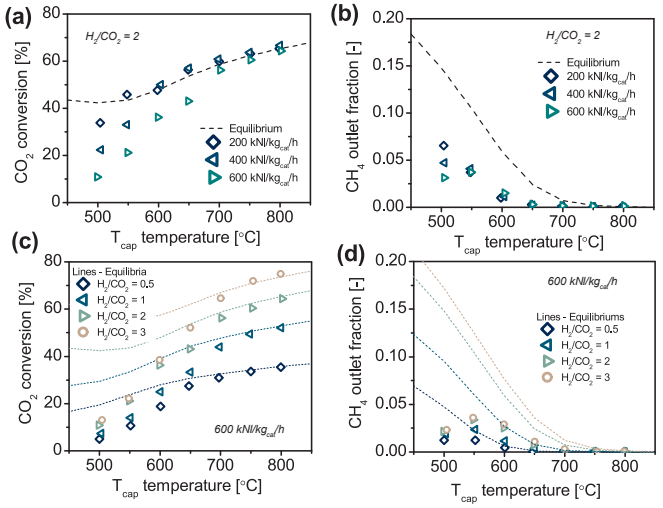

Fig. 9. (a) CO_2 conversion and (b) CH_4 outlet fraction during eRWGS runs with different space velocity: GHSV = 200, 400 and 600 kNl/kg_{cat}/h with a fixed H_2/CO_2 feed ratio of 2; (c) CO_2 conversion and (d) CH_4 outlet fraction from eRWGS runs with different H_2/CO_2 feed ratio of 0.5, 1, 2 and 3 at a fixed GHSV = 600 kNl/kg_{cat}/h. Experiments were carried out with 1 %Rh/Al_2O_3 washcoated SiSiC foam (L_{foam} = 8 cm) with catalyst density of 13 g/L, ambient pressure.

4. Conclusions

We have proposed and successfully demonstrated the electrified CO_2 reforming of methane (eCRM) and the electrified reverse water–gas shift (eRWGS) reactions for CO_2 valorization, based on direct Joule heating of catalytically activated open-cell foams. Such a reactor concept, relying on porous SiSiC foams that act as catalyst supports as well as heating substrates, allows to reach CO_2 conversion approaching equilibrium in a wide range of operating conditions. The eRWGS process exhibits great potential to achieve low specific energy consumptions for CO_2 conversion: calculations showed that 0.7 kWh/Nm^3_{CO2} could be reached assuming an overall adiabaticity of 95% and 90% recovery of the sensible heat. Moreover, hardly any CH_4 could be detected in the products during the eRWGS runs above 675 °C. With a H_2-rich feed, a CO_2 conversion of 94.2% was achieved. Furthermore, the Joule-heated Rh/Al_2O_3-coated foam exhibited excellent catalytic and electrical stability for more than 75 h. By replacing fuel combustion heating with Joule heating based on renewable electric energy, both processes are encouraging solutions for CO_2 valorization while drastically reducing the carbon footprint for downstream chemical productions. By considering the potential for compact small-scale reactor design as a result of enhanced heat and mass transfer properties, combined with the fast heat transfer dynamics of Joule heating, the proposed electrified CO_2 valorization concept can be regarded as a promising option to mitigate the

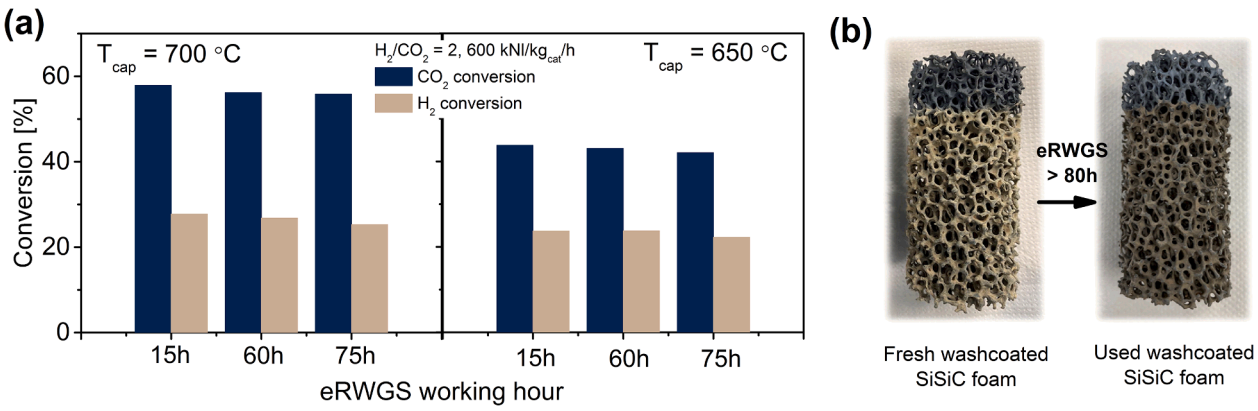

Fig. 10. Stability of the washcoated SiSiC foam in eRWGS experiments: (a) CO_2 and H_2 conversions from eRWGS working hours of 15 h, 60 h and 75 h, experiments were carried out at T_{cap} of 700 °C and 650 °C, H_2/CO_2 feed ratio of 2, 600 kNl/kgcat/h, ambient pressure, note that eRWGS runs at varied conditions such as diffirent space velocity, diffirent H_2/CO_2 feed ratio were carried out among those times. (b) Fresh SiSiC foam and used SiSiC foam after at least 80 h on eRWGS stream with different experimental feed conditions. 1%Rh/Al_2O_3 washcoated SiSiC foam (L_{foam} = 8 cm) with catalyst density of 13 g/L.

intermittent nature of renewable sources by storing the excess energy in chemicals.

The proposed electrified foam-based reactor system is in principle applicable to the Ni-based catalysts commonly reported for both reforming and reverse-water gas shift reactions. However, the Rh-based catalysts are known to offer higher activity per catalyst volume/mass. Combined with the excellent stability of the catalyst, and with the significantly reduced heat and mass transfer limitations, the Joule-heated Rh-catalyst washcoated foam reactor thus provides significant advantages in terms of process intensification, particularly in view of the design of compact small-scale reactors.

Declaration of Competing Interest

The authors declare that they have no known competing financial interests or personal relationships that could have appeared to influence the work reported in this paper.

Data availability

Data will be made available on request.

Acknowledgements

This work has received fundings from MIUR Progetti di Ricerca di Rilevante Interesse Nazionale (PRIN) Bando 2020 under the project (2020N38E75-"PLUG-IN"), and the European Research Council (ERC) under the European Union's Horizon 2020 research and innovation programme (GA No. 694910-'INTENT'). The authors thank Federico Nicolini and Tiancheng Wang for their assistance in the present work. Daniele Marangoni is gratefully acknowledged for technical support to catalyst testing.

Appendix A. Supplementary data

Supplementary data to this article can be found online at https://doi.org/10.1016/j.cej.2023.143154.

References

[1] International Energy Agency, Global Hydrogen Review 2021, www.iea.org, accessed December 1, 2022.
[2] R.M. Bown, M. Joyce, Q. Zhang, T.R. Reina, M.S. Duyar, Identifying commercial opportunities for the reverse water gas shift reaction, Energ. Technol. 9 (11) (2021) 2100554.
[3] E. Schwab, A. Milanov, S.A. Schunk, A. Behrens, N. Schödel, Dry reforming and reverse water gas shift: alternatives for syngas production? Chem. Ing. Tech. 87 (4) (2015) 347–353.
[4] D. Pakhare, J. Spivey, A review of dry (CO_2) reforming of methane over noble metal catalysts, Chem. Soc. Rev. 43 (22) (2014) 7813–7837.
[5] A.d. Pee, D. Pinner, O. Roelofsen, K. Somers, Decarbonization of industrial sectors: the next frontier, McKinsey (2018).
[6] G.P. Thiel, A.K. Stark, To decarbonize industry, we must decarbonize heat, Joule 5 (3) (2021) 531–550.
[7] Z.J. Schiffer, K. Manthiram, Electrification and decarbonization of the chemical industry, Joule 1 (1) (2017) 10–14.
[8] S.T. Wismann, J.S. Engbæk, S.B. Vendelbo, F.B. Bendixen, W.L. Eriksen, K. Aasberg-Petersen, C. Frandsen, I. Chorkendorff, P.M. Mortensen, Electrified methane reforming: A compact approach to greener industrial hydrogen production, Science 364 (6442) (2019) 756–759.
[9] K.M. Van Geem, V.V. Galvita, G.B. Marin, Making chemicals with electricity, Science 364 (6442) (2019) 734–735.
[10] K.M. Van Geem, B.M. Weckhuysen, Toward an e-chemistree: Materials for electrification of the chemical industry, MRS Bull. (2022) 1–10.
[11] E. Klemm, C.M. Lobo, A. Löwe, V. Schallhart, S. Renninger, L. Waltersmann, R. Costa, A. Schulz, R.U. Dietrich, L. Möltner, CHEMampere: Technologies for sustainable chemical production with renewable electricity and CO_2, N_2, O_2, and H_2O, The, Can. J. Chem. Eng. 100 (2022) 2736–2761.
[12] R. Küngas, Electrochemical CO_2 reduction for CO production: comparison of low- and high-temperature electrolysis technologies, J. Electrochem. Soc. 167 (4) (2020), 044508.
[13] Haldor Topsoe, Produce your own carbon monoxide tailored to your business-eCOs™, www.topsoe.com/processes/carbon-monoxide, Accessed March 26, 2023.
[14] A.I. Stankiewicz, H. Nigar, Beyond electrolysis: old challenges and new concepts of electricity-driven chemical reactors, React. Chem. Eng. 5 (6) (2020) 1005–1016.
[15] M. Ambrosetti, A perspective on power-to-heat in catalytic processes for decarbonization, Chemical Engineering and Processing-Process Intensification 182 (2022), 109187.
[16] W. Wang, S. Zhao, X. Tang, C. Chen, H. Yi, Electrothermal Catalysis for heterogeneous reaction: Mechanisms and design strategies, Chem. Eng. J. (2022), https://doi.org/10.1016/j.cej.2022.140272.
[17] I. Dincer, 1.7 energy and exergy efficiencies, Comprehensive Energy Systems; Dincer, I., Ed.; Elsevier: Oxford, UK (2018) 265-339.
[18] Q. Dong, Y. Yao, S. Cheng, K. Alexopoulos, J. Gao, S. Srinivas, Y. Wang, Y. Pei, C. Zheng, A.H. Brozena, Programmable heating and quenching for efficient thermochemical synthesis, Nature 605 (7910) (2022) 470–476.
[19] S.T. Wismann, J.S. Engbæk, S.B. Vendelbo, W.L. Eriksen, C. Frandsen, P. M. Mortensen, I. Chorkendorff, Electrified methane reforming: Elucidating transient phenomena, Chem. Eng. J. 425 (2021), 131509.
[20] P. Du, R. Wang, B. Deng, X. He, Y. Long, C. Yang, Z. Wang, B. Ge, K. Huang, R. Zhang, In-situ Joule-heating drives rapid and on-demand catalytic VOCs removal with ultralow energy consumption, Nano Energy 102 (2022), 107725.
[21] G. Cao, R.M. Handler, W.L. Luyben, Y. Xiao, C.-H. Chen, J. Baltrusaitis, CO_2 conversion to syngas via electrification of endothermal reactors: Process design and environmental impact analysis, Energ. Conver. Manage. 265 (2022), 115763.
[22] L. Basini, F. Furesi, M. Baumgärtl, N. Mondelli, G. Pauletto, CO_2 capture and utilization (CCU) by integrating water electrolysis, electrified reverse water gas shift (E-RWGS) and methanol synthesis, J. Clean. Prod. 377 (2022), 134280.
[23] X. Mei, X. Zhu, Y. Zhang, Z. Zhang, Z. Zhong, Y. Xin, J. Zhang, Decreasing the catalytic ignition temperature of diesel soot using electrified conductive oxide catalysts, Nat. Catal. 4 (12) (2021) 1002–1011.
[24] Q. Xiong, X. Zhu, R. He, X. Mei, Y. Zhang, Z. Zhong, W. Zhao, W. Nie, J. Zhang, Local Joule heating targets catalyst surface for hydrocarbon combustion, J. Ind. Eng. Chem. 117 (25) (2023) 273–281.

[25] M.B. Glaser, G. Thodos, Heat and momentum transfer in the flow of gases through packed beds, AIChE J 4 (1) (1958) 63–68.
[26] S. Renda, M. Cortese, G. Iervolino, M. Martino, E. Meloni, V. Palma, Electrically driven SiC-based structured catalysts for intensified reforming processes, Catal. Today 383 (2020) 31–43.
[27] M. Rieks, R. Bellinghausen, N. Kockmann, L. Mleczko, Experimental study of methane dry reforming in an electrically heated reactor, Int. J. Hydrogen Energy 40 (46) (2015) 15940–15951.
[28] V. Balakotaiah, R.R. Ratnakar, Modular reactors with electrical resistance heating for hydrocarbon cracking and other endothermic reactions, AIChE J 68 (2) (2022) e17542.
[29] G. Pauletto, A reactor with an electrically heated structured ceramic catalyst, European Patent EP 3895795A1 (2020).
[30] Q. Wang, Y. Ren, X. Kuang, D. Zhu, P. Wang, L. Zhang, Electrically heated monolithic catalyst for in-situ hydrogen production by methanol steam reforming, Int. J. Hydrogen Energy 48 (2) (2023) 514–522.
[31] S.T. Wismann, K.E. Larsen, P. Mortensen, Electrical reverse shift: Sustainable CO_2 valorization for industrial scale, Angew. Chem. 134 (8) (2022) e202109696.
[32] S.T. Wismann, J.S. Engbæk, S.B. Vendelbo, W.L. Eriksen, C. Frandsen, P. M. Mortensen, I. Chorkendorff, Electrified methane reforming: Understanding the dynamic interplay, Ind. Eng. Chem. Res. 58 (51) (2019) 23380–23388.
[33] L. Zheng, M. Ambrosetti, D. Marangoni, A. Beretta, G. Groppi, E. Tronconi, Electrified methane steam reforming on a washcoated SiSiC foam for low-carbon hydrogen production, AIChE J 69 (1) (2023) e17620.
[34] L. Dou, C. Yan, L. Zhong, D. Zhang, J. Zhang, X. Li, L. Xiao, Enhancing CO_2 methanation over a metal foam structured catalyst by electric internal heating, Chem. Commun. 56 (2) (2020) 205–208.
[35] A. Badakhsh, Y. Kwak, Y.-J. Lee, H. Jeong, Y. Kim, H. Sohn, S.W. Nam, C.W. Yoon, C.W. Park, Y.S. Jo, A compact catalytic foam reactor for decomposition of ammonia by the Joule-heating mechanism, Chem. Eng. J. 426 (15) (2021), 130802.
[36] M. Ambrosetti, A. Beretta, G. Groppi, E. Tronconi, A numerical investigation of electrically-heated methane steam reforming over structured catalysts, Frontiers in Chemical Engineering 3 (2021), 747636.
[37] L. Zheng, M. Ambrosetti, F. Zaio, A. Beretta, G. Groppi, E. Tronconi, Direct electrification of Rh/Al_2O_3 washcoated SiSiC foams for methane steam reforming: An experimental and modelling study, Int. J. Hydrogen Energy 48 (2023) 14681.
[38] M. Maestri, D.G. Vlachos, A. Beretta, G. Groppi, E. Tronconi, Steam and dry reforming of methane on Rh: Microkinetic analysis and hierarchy of kinetic models, J. Catal. 259 (2) (2008) 211–222.
[39] L. Dietz, S. Piccinin, M. Maestri, Mechanistic Insights into CO_2 activation via reverse water-gas shift on metal surfaces, J. Phys. Chem. C 119 (9) (2015) 4959–4966.
[40] M. Nagai, K. Nakahira, Y. Ozawa, Y. Namiki, Y. Suzuki, CO_2 reforming of methane on Rh/Al_2O_3 catalyst, Chem. Eng. Sci. 62 (18–20) (2007) 4998–5000.
[41] T. Mathew, S. Saju, S.N. Raveendran, Survey of heterogeneous catalysts for the CO_2 reduction to CO via reverse water gas shift, In Engineering Solutions for CO_2 Conversion; Reina, T.R., Arellano-Garcia, H., Odriozola, J.A., Eds.; Wiley: Hoboken, NJ, USA, 2021; Chapter 12; pp. 281–316. (2021).
[42] M. Bracconi, M. Ambrosetti, M. Maestri, G. Groppi, E. Tronconi, A fundamental investigation of gas/solid mass transfer in open-cell foams using a combined experimental and CFD approach, Chem. Eng. J. 352 (2018) 558–571.
[43] K. Wang, Y. Zeng, W. Lin, X. Yang, Y. Cao, H. Wang, F. Peng, H. Yu, Energy-efficient catalytic removal of formaldehyde enabled by precisely Joule-heated Ag/Co_3O_4@mesoporous-carbon monoliths, Carbon 167 (2020) 709–717.
[44] Q. Zhang, M. Nakaya, T. Ootani, H. Takahashi, M. Sakurai, H. Kameyama, Simulation and experimental analysis on the development of a co-axial cylindrical methane steam reformer using an electrically heated alumite catalyst, Int. J. Hydrogen Energy 32 (16) (2007) 3870–3879.
[45] K. Yu, C. Wang, W. Zheng, D.G. Vlachos, Dynamic electrification of dry reforming of methane with in situ catalyst regeneration, ACS Energy Lett. 8 (2023) 1050–1057.
[46] Q. Xiong, X. Zhu, R. He, X. Mei, Y. Zhang, Z. Zhong, W. Zhao, W. Nie, J. Zhang, Local Joule heating targets catalyst surface for hydrocarbon combustion, J. Ind. Eng. Chem. 117 (2023) 273–281.
[47] D.D. Wang, S. Li, L. Gao, Asme, A novel coal gasfication system through thermochemical regenerative process of syngas sensible heat to enhance cold gas efficiency, 11th ASME International Conference on Energy Sustainability, Charlotte, NC, 2017.
[48] G. Natrella, A. Borgogna, A. Salladini, G. Iaquaniello, How to give a renewed chance to natural gas as feed for the production of hydrogen: Electric MSR coupled with CO_2 mineralization, Cleaner Eng. Technol. (2021), 100280.
[49] D.J. Jovan, G. Dolanc, Can green hydrogen production be economically viable under current market conditions, Energies 13 (24) (2020) 6599.
[50] D. Heyl, U. Rodemerck, U. Bentrup, Mechanistic study of low-temperature CO_2 hydrogenation over modified Rh/Al_2O_3 catalysts, ACS Catal. 6 (9) (2016) 6275–6284.
[51] T. Wind, H. Falsig, J. Sehested, P. Moses, T. Nguyen, Comparison of mechanistic understanding and experiments for CO methanation over nickel, J. Catal. 342 (2016) 105–116.